Review

PEM Fuel Cell Emulators: A Review

Ángel Hernández-Gómez [1], Diego Langarica-Cordoba [1], Panfilo R. Martinez-Rodriguez [1], Damien Guilbert [2,*], Victor Ramirez [3,4,*] and Belem Saldivar [5]

1 School of Sciences, Universidad Autónoma de San Luis Potosí (UASLP), San Luis Potosí 78295, Mexico; angel-hernandez-1@hotmail.com (Á.H.-G.); diego.langarica@uaslp.mx (D.L.-C.); panfilo.martinez@uaslp.mx (P.R.M.-R.)
2 Group of Research in Electrical Engineering of Nancy (GREEN), Université de Lorraine, F-54000 Nancy, France
3 Department of Renewable Energy, Centro de Investigación Científica de Yucatán (CICY), Yucatán P. C. 97205, Mexico
4 Consejo Nacional de Ciencia y Tecnología (CONACYT), Mexico City P. C. 03940, Mexico
5 Department of Automatic Control, CINVESTAV-IPN, Av. Instituto Politécnico Nacional 2508, Mexico City 07360, Mexico; belem.saldivar@cinvestav.mx
* Correspondence: damien.guilbert@univ-lorraine.fr (D.G.); victor.ramirez@cicy.mx (V.R.)

Abstract: Proton exchange membrane fuel cell (PEMFC) emulators are feasible solutions for conducting low-cost and safe developments. These types of systems have attracted the attention of global PEMFC manufacturers and research groups over the last few years. Owing to these emulators, it has been possible to develop and optimize PEMFC systems including power electronics and control without the need to use or damage a real PEMFC. However, despite the importance of PEMFC emulators in research, reported studies on this topic remain scarce. For this reason, this review describes the main characteristics and different types of PEMFC emulators (i.e., pseudo and electronic emulators), providing a basis for new emulator prototypes. Additionally, in this paper, the mathematical models that complement PEMFC emulators are presented (i.e., these models and emulators generate reliable measurements compared with real PEMFC systems). Examples of electronic circuit designs based on mathematical models (electrical and heat) are also presented to give some insight into the construction of new PEMFC emulators. Therefore, this paper proposes tools for the construction of new PEMFC emulators to boost the development of this technology.

Keywords: circuit electronic modeling; current ripple; DC–DC converter; hardware in a loop; PEMFC; PEMFC emulators

1. Introduction

Due to the high costs of fossil fuels and growing concerns about greenhouse gas emissions, researchers are looking for renewable energy sources, with the aim of sustainability with accessible cost, high efficiency, and low-environmental-impact power conversion. Therefore, the interest in power-generating systems such as photovoltaics, wind turbines, and fuel cells (FCs) has increased. However, the intermittency and instability of renewable energies, such as solar and wind, have produced challenges for the stable operation of electrical systems, creating temporal and spatial gaps between energy consumption by end users and energy availability. Therefore, additional energy storage technology is needed as an effective means to help achieve stable and efficient renewable energy operation [1]. FC systems are not subject to intermittent restrictions, making them safer and more reliable. Additionally, FC systems have been shown to be sources of clean energy, environmentally friendly, and sustainable due to their higher energy efficiency, reduced emissions, and high energy density [2,3].

The primary function of FCs is to convert chemical energy from gaseous fuel into electricity. FCs can also serve as substitute stationary and mobile power sources [4].

Today, different manufacturers offer many options and types of FCs. They can be classified according to their specific characteristics, such as the type of fuel used, the reaction temperature, and the electrochemical material used [5]. In addition, the main FCs reported in the literature are proton exchange membrane (PEMFCs), direct methanol, solid oxide, molten carbonate, phosphoric acid, alkaline, and microbial FCs [6,7]. In the field of both stationary and mobile applications, PEMFCs are among the most widely used and promising. This is due to their main features, which are quick and silent start-up operation, robustness, and a relatively low operating temperature range, which is, in general, between 60 and 80 °C [8,9].

Despite the significant technological advancements in PEMFC in recent years, issues such as their cost, size, weight, and complexity of peripheral devices are still of interest for research because the PEMFC system is intricate, involving several physical phenomena, including thermal, electrochemical, and electrical aspects. The PEMFC stack needs several auxiliary components for its correct operation, such as a humidification system, a cooling system, an air management system, and a hydrogen supply system. To enhance PEMFC performance, it is necessary to study, develop, and optimize every auxiliary component. This will allow the optimization of both the PEMFC stack and the powerful nonlinear interactions that exist among its components [10]. However, the acquisition of PEMFC system components and the considerable amount of labor required to assemble the usual complex PEMFC systems result in very high costs [11]. Therefore, due to the high costs involved, many researchers have performed studies based on numerical simulations using computational fluid dynamics (CFD), which is a branch of fluid mechanics that uses numerical analysis and data structures to analyze and solve problems involving fluid flows in PEMFCs. However, the experimental hardware is ignored when using simulation (software) only, but this hardware is important in studying the behavior of the PEMFC in a complete system (microgrid). For this reason, hardware capable of accurately imitating the behavior of a PEMFC can allow experimentation without the use of a real PEMFC, at least for the first experimental stages. These hardware systems are called emulators or real-time simulatosr [12].

A real PEMFC can be replaced with an emulator, allowing for the study and configuration of the remaining PEMFC components (auxiliaries, power electronics interfaces, loads, etc.) [13]. The final stage involves replacing the emulator with the real PEMFC once the system has been thoroughly examined and confirmed. In this way, all risks of damage to the system are reduced, and money, time, and space are saved [14].

Mathematical models are essential for the development of PEMFC emulators [15]. However, despite the wide variety of models developed for PEMFCs [16–25], those that are most suited to the purpose of emulator development are the equivalent electronic circuit models (ECMs) because these models are fit to describe the electrical behavior of a PEMFC or how the PEMFC interacts with the associated electrical systems and power conditioning circuits such as power electronics [26]. In addition, ECMs aid with electronic interface design and control and reliability test analysis [27,28]. Two types of ECMs have been reported: dynamic and passive models [26]. Chemical and thermodynamic processes must both be considered in a dynamic model. Consequently, it is possible to construct an optimal system in terms of efficiency and cost by understanding the special properties of the PEMFC [29,30]. Furthermore, power converter performance, transient response, and efficiency can be improved using a dynamic model, allowing for the creation of control systems that are appropriate for the load demand [31]. Passive models can be used to predict the performance and degradation of a PEMFC while it is in standby mode. This mode is appropriate for uninterruptible power systems when dependability is crucial and the PEMFC is idle for the majority of the time [26].

With the development of ECMs for PEMFCs, the construction of emulators has become viable, because it depends on the construction and implementation of an electronic circuit into the system. Although some authors have already developed and implemented emulators, this field is still developing due to the few reported studies in the literature.

The reported emulators can be classified as pseudo emulators [10,32] and electronic emulators, the latter of which are divided into electrical [11,12,14,15,33–66] and heat emulators [11,36,55,67].
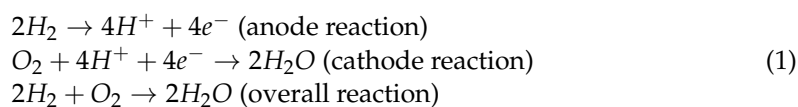
Particularly for electrical emulators, different investigations have been carried out for their design, construction, and validation. In [59–61,63,66], electrical emulators have been developed for 10 W, 1.2 kW, 3 kW, and 5 kW PEMFC systems. Additionally, the reported controllers for electric emulators have been realized on hardware platforms based on DC–DC buck converters, the control strategies of which are mainly based on PI controllers [49] and fuzzy control [54], among others. This kind of system is typically implemented on digital platforms using digital signal processors (DSPs) or dSPACE control boards [10,14,57,62] and field programmable gate arrays (FPGAs) systems [61]. For the validation of the emulators, in addition to performing a comparison of data taken from a real PEMFC, the hardware-in-a-loop (HIL) system has been successfully used [37,40–42,44,46–48,56]. As a result, due to the few reported studies and the importance of PEMFC emulators for the investigation and optimization of PEMFC systems, this review aims to provide a guide for the development of future emulators for PEMFCs.

This paper is composed of six sections. After pointing out the motivations and current state of the art regarding this review in the Introduction, in Section 2, a summary of the basic PEMFC characteristics is presented. After that, the different types of emulators, controllers, and validation methods are explained in Section 3. In Section 4, mathematical models of PEMFC emulators are described. Because the design of electronic circuits is important for the construction and implementation of an electronic emulator PEMFC, examples of these designs are presented in Section 5. Finally, in Section 6, a discussion is given.

2. The Basic Operation of PEMFCs

A lot of research has been conducted to make PEMFCs that are highly reliable and efficient for use in various applications such as portable power source devices and stationary or mobile applications. Owiwng to the development of computational fluid mechanics and working memory resources in computers capable of simultaneously solving many equations, recent advances have been made, particularly in materials and current density, which will eventually increase power density, device efficiency, and reliability [68]. In addition, compared with heat engines and when used in modular power generation, PEMFCs are more efficient [69].

A PEMFC is formed by a proton exchange membrane sandwiched between two electrodes (anode and cathode). Due to its unique characteristic, the membrane only permits protons to travel through while blocking electrons, especially perfluoro sulfonic acid membrane materials represented by Nafion and other sulfonated polymers [70]. In particular, Nafion contains a hydrophobic polytetrafluoroethylene (PTFE) backbone and a hydrophilic sulfonic acid group as the end group of the side chain. The membrane phase separates only after hydration, forming channels for proton conduction [71]. As hydrogen gas travels over the anode, it splits into hydrogen protons and electrons with the aid of a catalyst. Electricity is produced by the flow of protons via the proton exchange membrane to the cathode and the flow of electrons through an external circuit. Water is created when oxygen and hydrogen protons and electrons pass through the cathode, as shown in Figure 1. The reactions in a PEMFC are given by [72]:

$$
\begin{aligned}
&2H_2 \rightarrow 4H^+ + 4e^- \text{ (anode reaction)} \\
&O_2 + 4H^+ + 4e^- \rightarrow 2H_2O \text{ (cathode reaction)} \\
&2H_2 + O_2 \rightarrow 2H_2O \text{ (overall reaction)}
\end{aligned}
\tag{1}
$$

The typical characteristics of PEMFCs are usually described by the polarization curve, which is a function depending on the voltage and current of the cell. Due to PEMFC electrical impedance, ineffective transport of the reactant gas, and slow reaction rate, the voltage decreases as more current is extracted from it. Low-load operation is desirable because a lower voltage indicates a lower-efficiency PEMFC. However, FC size and weight

are increased as a result. Furthermore, mobile applications that require frequent load changes cannot operate at low loads all the time. The polarization curve varies with the operating conditions, including pressure, temperature, partial pressure of reactants, and membrane humidity [69].
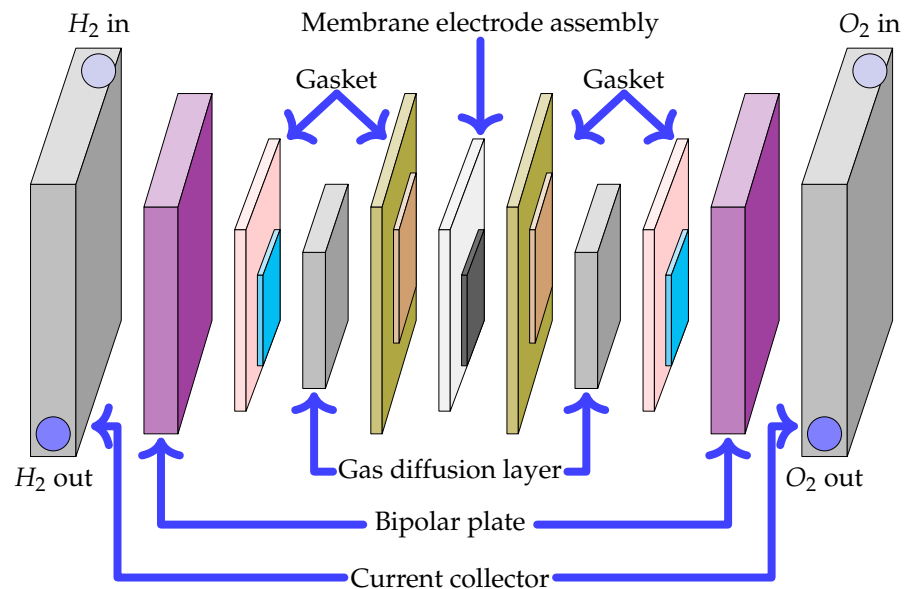

Figure 1. Scheme of a basic PEMFC.

As shown in Figure 1, to form a complete FC system, the PEMFC stack needs several ancillary parts in addition to the four main flow subsystems: an anode hydrogen supply system, a cathode air supply system, a humidifier, and a cooler that maintains the temperature and humidity level of the PEMFC. To avoid constant heating and ensure fast system transient response, safe shutdown, system robustness, and the ability to adapt to power changes, the main parameters that need to be regulated are reagent flow rate, total pressure, partial pressure of the reagent, membrane, temperature, and humidity. The key control mechanisms are the water pump for temperature regulation, the humidifier for humidity management, the hydrogen flow and pressure-regulating valve, and the compressor motor for pressure regulation and airflow. It is worth mentioning that changes in one parameter influence the others. For instance, an increase in airflow velocity can raise the air pressure, but it can also change the amount of heat and steam that enters and leaves the stack, influencing the temperature and humidity of the stack and the membrane [57,69]. Thus, this is why PEMFC systems are complex.

3. Types of PEMFC Emulators

Emulators are frequently employed in renewable energy systems because these electrical-power-generating systems are expensive, typically have security requirements, use chemical reagents, and exhibit unpredictable behavior [38]. Emulators for different types of fuel cells have already been reported in the literature [73–75]. However, as mentioned in the Introduction, this review is focused on PEMFC emulators.

PEMFC emulators are designed to reproduce certain characteristics of this type of FC. Thus, experiments and studies of these characteristics have been carried out mimicking real performance without the need for a PEMFC [5,10]. Currently, an efficiency of 97% has been achieved for PEMFC emulators [5]. The initial step in simulating PEMFC systems is establishing the emulator's implementation characteristics while taking into account the PEMFC application and objective. It is recommended to use digital processing systems as they allow quick and easy modifications of the algorithm because the emulation system must be frequently modified [38]. Additionally, for emulator lifetime purposes, several factors must be taken into account, such as the build quality, the type of components,

the way it is used and maintained, the deployment environment, and the frequency of use. Additionally, PEMFC emulators are subject to wear and tear and possible failure due to continued use or the passage of time. In this section, different types of PEMFC emulators are briefly described.

3.1. Pseudo Emulators

PEMFC pseudo emulators are designed to replace computer models of PEMFCs with a real small PEMFC. With the use of scaling rules, the emulator is capable of imitating the behavior of a full-size PEMFC using this method. Pseudo emulators have the benefit of scaling currents and voltages in response to the emulator's actual load, which enables the testing of systems of any size [32]. However, this type of emulator requires suitable PEMFC auxiliary components [10].

3.2. Electrical Emulators

By programming a DC power source, a PEMFC electrical emulator can be quickly and easily created. Nevertheless, these DC power sources frequently have current and voltage ranges that are not the same as those needed to replicate a particular PEMFC model [63]. Therefore, a DC transformer based on a noninverting DC–DC buck-boost converter (generally buck converter) is necessary between the load and the DC power source to modify the voltage or current of the emulated PEMFC [34,63].

Considering this electronic emulator development, the use of control strategies and implementation methods is necessary for the reliable validation of PEMFC electrical emulators. For this reason, this subsection also presents some control techniques reported in the literature.

Control Strategies and Implementation Methods for Electric Emulators

Proportional-integral (PI) controllers. PI controllers have been applied to control electric emulators based on buck converters. This controller creates a control signal for a pulse width modulator (PWM), which provides the gate signal pulses of a MOSFET switch by comparing the output voltage to the PEMFC's reference voltage [49].

Fuzzy controller. These models have been proven to be suitable for the implementation of PEMFC emulators and the development of the simulation of control strategies due to their simplicity, short processing time, and extensive knowledge of implementation techniques [54]. The fuzzy relational model, neural-network-based fuzzy model, T-S fuzzy model, and fuzzy basis function-based model are a few modeling methods based on fuzzy reasoning that have been presented in recent years [76]. In particular, for PEM emulators, given their computing limitations, a low-cost digital processing device is created to apply a fuzzy-based model in the emulator and meet the needs of real-time processing [54].

Digital signal orocessor (DSP) and dSPACE. In the application of PEMFC emulators, a linear power amplifier linked to a DC–DC converter or directly to a load uses the output voltage from dSPACE as a reference control. The dSPACE protoboard has a digital-to-analog converter to connect the reference cell voltage from the PEMFC model to the power amplifier, an integrated DSP where the PWM controller is loaded, an analog-to-digital converter to read the measurement inputs from the sensors, and a digital input/output port for sending and receiving PWM signals [10,14,57,62].

Field-programmable gate array (FPGA). After production, an FPGA-integrated circuit can be configured by a customer or designer. In PEM emulator applications, the digital controller that simulates the PEMFC stack being tested is part of the FPGA system. The controller receives the digitized output voltage from the digitized current stream. The power stage provides the interface between the charging device and the emulator system. The controller samples the FC current while simulating the voltage across the PEMFC. Additionally, using the controller, it is possible to establish the initial temperature of the PEMFC stack being tested as well as the ambient temperature and determine the temperature of the stack using current samples [61].

3.3. Heat Emulators

Studies on heat emulators based on electronic circuits are very scarce [11,36,67]. Electric plate heaters were used to generate the necessary amount of heat, emulating this parameter from the PEMFC stack. In addition, a collection of copper blocks was used to imitate a PEMFC stack's internal heat capacity. To do this, the right number of blocks was selected to correspond to the comparable heat capacity of an actual PEMFC [11]. In the studies reported so far, the PEMFC heat emulators have been controlled by a microcontroller [11,36,67].

3.4. HIL Method

A PEMFC emulator can be used for HIL applications to test and validate the design of PEMFC systems [44]. The HIL method is a simulation/emulation process that connects software models of other system components with the hardware being tested or a reduced version of it [32]. Thus, using the HIL method, PEMFC auxiliaries can be tested and improved in real time with a PEMFC emulator without the risk of the PEMFC stack being damaged and at a low operating cost [44].

Figure 2 presents a diagram that summarizes the different types of reported emulators and the main characteristics of their design and construction.
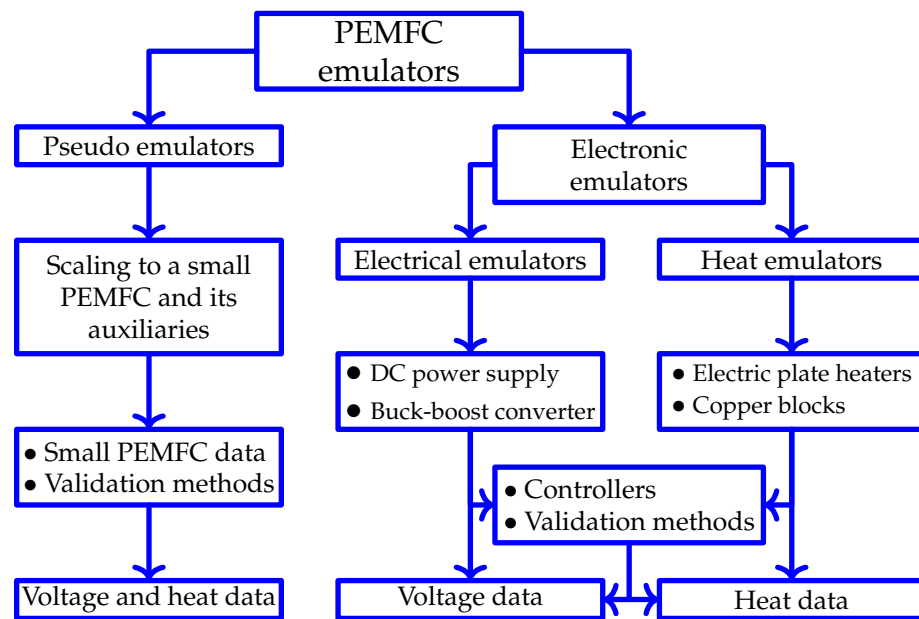

Figure 2. Diagram of the different types of emulators and the main characteristics of their design and construction.

4. Mathematical Model

The mathematical models used for the development of simulations, electronic circuits, and emulators are presented in this section.

4.1. Voltage–Current Models

Generally, the polarization curve of a PEMFC is non-inear and expressed in terms of PEMFC power P_{fc}:

$$P_{fc} = V_{fc} \cdot I_{fc} \tag{2}$$

where V_{fc} is the voltage (V), and I_{fc} is the electrical current (A) of the PEMFC. The voltage V_{fc} is usually expressed in terms of Nernst's voltage E_{th} and the voltage drops: activation V_{act}, ohmic V_{ohm}, and concentration V_{con} [14,77]:

$$V_{fc} = E_{th} - V_{ohm} - V_{act} - V_{con}, \tag{3}$$

Nernst's voltage E_{th}. The difference between the reactant products and the Gibbs free energy yields Nernst's voltage, also known as the open-circuit voltage, which is the highest power obtained by one cell and corresponds to the exchanged Gibbs free energy. The following equation can be used to describe it [78,79]:

$$E_{th} = E_0 + B_1 \cdot (T_0 - T) + B_2 \cdot T \cdot \ln \left[\frac{P_{H_2} \cdot P_{O_2}^{1/2}}{P_{H_2O}} \right], \tag{4}$$

where T_0 and T are initial and cell temperatures (K), respectively; P_{H_2}, P_{O_2}, and P_{H_2O} are hydrogen, oxygen, and water pressures (atm), respectively; E_0 is the reference voltage (V); B_1 and B_2 are positive constants [77]. It should be noted that the initial pressure values in a PEMFC can be measured using differential pressure sensors, which are usually placed in the inlet and outlet flow channels of the gases. Thus, the pressure difference can provide information about the flow and resistance in a cell.

Ohmic voltage drop V_{ohm}. The ohmic voltage drop results from the resistances of the polymer membrane to proton transfer and of the electrode and collector plate to electron transfer [77–79].

$$V_{ohm} = I_{fc} \cdot R_{ohm}, \tag{5}$$

where R_{ohm} is the internal electrical resistance (Ω). The membrane conductivity σ_m can be used to express the ohmic resistance (cm·Ω^{-1}).

$$R_{ohm} = \frac{t_m}{\sigma_m}, \tag{6}$$

where t_m is the membrane thickness (cm). σ_m can be expressed as a function of membrane water content λ_m and T.

$$\sigma_m = (b_1 \cdot \lambda_m - b_2) \cdot \exp \left[b_3 \cdot \left(\frac{1}{T_0} - \frac{1}{T} \right) \right], \tag{7}$$

where b_1, b_2, and b_3 are constants and are usually assessed empirically.

Activation voltage drop V_{act}. The requirement to transfer electrons, and break and create chemical bonds in the anode and cathode causes the drop in activation voltage. Driving the chemical reaction that moves the electrons to and from the electrodes uses up some of the available energy. Both the anode and cathode of a PEMFC electrode experience activation voltage. Yet, compared with the reaction of oxygen at the anode, the hydrogen oxidation process occurs quickly [77]. V_{act} can be expressed as (8) [57,72].

$$V_{act} = \left(\frac{R \cdot T}{\alpha \cdot z \cdot F} \right) \cdot \ln \left(\frac{I_{fc}}{I_0} \right) = b_4 + T \cdot [b_5 + b_6 \cdot \ln(I_{fc})], \tag{8}$$

where R is the universal gas constant (J · mol^{-1} · K^{-1}), α is the electron transfer coefficient, z is the number of participating electrons, F is Faraday's constant (C · mol^{-1}), and I_0 is the exchange current (A). b_4, b_5, and b_6 are the constants in the Tafel equation.

Concentration voltage drop V_{con}. The concentration gradients created by mass diffusions from the flow channels to the reaction sites are represented by the concentration voltage drop (catalyst area). High current densities, lethargic transport of reactants and products to and from the reaction sites, and a water film coating the catalyst surfaces on

the anode and cathode are the causes of this voltage drop [77]. V_{con} can be expressed by (9) [11,72].

$$V_{con} = \left(\frac{R \cdot T}{z \cdot F}\right) \cdot \ln\left(1 - \frac{I_{fc}}{I_{\max}}\right), \tag{9}$$

where I_{max} is the maximum operating current of a PEMFC (A) with a restriction established by concentration losses.

4.2. Voltage–Current ECMs

Researchers conducted an electrochemical analysis to develop an ECM for a PEMFC, which is applicable for modeling power generation and its converters. Model parameters were determined using experimental polarization curves and electrochemical impedance spectroscopy, and simulation results were validated using these methods [28].

Nernst's voltage. This voltage can be emulated by a DC voltage source V_{ini} [80]. Thus, it is possible to establish the following equation:

$$E_{th} = V_{ini}. \tag{10}$$

Ohmic voltage drop. An equivalent resistance connected in series to the model PEMFC terminal can simulate this voltage. FC manufacturers provide the corresponding internal resistance value. However, it must be remembered that variations in operating temperature can cause changes in the resistance of the PEMFC [14]. Notice that V_{ohm} can be represented by (5) as well.

Activation and concentration voltage drops. These voltages are responsible for the complex dynamics of the circuit. The double-layer charge effect serves as the primary regulator of PEMFC dynamics. A capacitor can be used to represent the charge layer that corresponds to the electrolyte/electrode contact because it functions as storage for electrical charges. Each change in voltage necessitates a charging time (in the event of an increase in voltage) or a leakage period (in the event of a voltage decrease). The ohmic drop, whose change can be thought of as instantaneous, is unaffected by this time delay but the activation and concentration voltages are affected. Thus, modeling of the activation and concentration voltage drops as first-order delay dynamics is possible.

$$\frac{d(V_{act} + V_{con})}{dt} = \frac{1}{C} \cdot I_{fc} - \frac{1}{\tau} \cdot (V_{act} + V_{con}), \tag{11}$$

with a time constant $\tau = C \cdot R_a$. Given that the equivalent resistance R_a depends on the activation and concentration voltages as well as the load current, the time constant τ controls the dynamics changes depending on the load conditions:

$$\tau = C \cdot R_a = C \cdot \left(\frac{V_{act} + V_{con}}{I_{fc}}\right). \tag{12}$$

So, by using (5), (10) and (11), PEMFC voltage can be expressed as:

$$V_{fc} = V_{ini} - I_{fc} \cdot R_{ohm} - (V_{act} + V_{con}). \tag{13}$$

4.3. Heat and Temperature Models

The thermal dynamic response of a FC Q_{fc} is due to each cell layer's capacity to conduct heat. The following description fits this dynamic for each thermal control volume [57]:

$$\frac{dQ_{fc}}{dt} = \frac{dQ_c}{dt} - \frac{dQ_e}{dt} - \frac{dQ_{loss}}{dt}. \tag{14}$$

where the chemical reaction Q_c, the electrical output power Q_e, and the heat loss Q_{loss} are responsible for releasing the available power and can be estimated by (15) to (17), respectively [57].

$$\frac{dQ_c}{dt} = n_{H_2} \cdot \left(\Delta G_0 - R \cdot T \cdot \text{In} \left(P_{H_2} \cdot \sqrt{P_{O_2}} \right) \right), \tag{15}$$

$$\frac{dQ_e}{dt} = V_{fc} \cdot I_{fc}, \tag{16}$$

$$\frac{dQ_{loss}}{dt} = h \cdot N \cdot A_{cell} \cdot (T - T_r), \tag{17}$$

where n_{H_2} is the number of moles of hydrogen (mol), ΔG_0 is the Gibbs free energy (J·mol^{-1}), h is the coefficient of convective heat transfer (W· cm^{-2}·K^{-1}), N is the number of cells in the stack, and A_{cell} is the cell area (cm^2).

Finally, a PEMFC works at a constant temperature when $Q_{fc} = 0$; however, the temperature may increase or decrease during transitions according to (18) [81].

$$M \cdot C_s \cdot \frac{dT}{dt} = \frac{dQ_{fc}}{dt}, \tag{18}$$

where M is PEMFC mass (kg), and C_s is the equivalent average specific heat coefficient (J·kg^{-1}·K^{-1}).

4.4. Heat and Temperature ECMs

The heat emulator circuit is based on a controllable voltage source V_H and a resistive heater R_H. The heat generated is a direct function of V_H [11].

$$Q_{fc} = \frac{V_H^2}{R_H}. \tag{19}$$

In other words, V_H directly controls the magnitude of the emulated waste heat.

4.5. Electrochemical Models

In this subsection, the equations that complement the emulation of a PEMFC system are presented. The electric power of the stack P_S (W) is obtained via:

$$P_S = N \cdot P_{fc}. \tag{20}$$

The equations for calculating mass fractions are provided in this subsection due to their importance in PEMFC simulations. The equations used to calculate the mass fractions provided in this review are ordinary differential equations or 0D, which are validated by measuring the inputs and outputs of the masses in a PEMFC.

The hydrogen mass flow rate of oxygen m_{H_2} (kg·s^{-1}) can be obtained using (21) [81].

$$m_{H_2} = \left(\frac{M_{H_2}}{2 \cdot F} \right) \cdot \left(\frac{P_S}{V_{fc}} \right), \tag{21}$$

where M_{H_2} is the molar mass of hydrogen (Kg·mol^{-1}). Additionally, the hydrogen excess ratio μ_{H_2} is calculated as a function of the hydrogen mass flow rate entering anodes $m_{H_2,in}$ and m_{H_2} [57].

$$\mu_{H_2} = \frac{m_{H_2,in}}{m_{H_2}}, \tag{22}$$

The mass flow rate entering the anode channel $m_{H_2,in}$ is calculated using the hydrogen mass flow rate reacting in the PEMFC stack and the purge mass flow rate $m_{H_2,purge}$. Therefore, $m_{H_2,in}$ can be defined by [57]:

$$m_{H_2,in} = m_{H_2} - m_{H_2,purge}. \tag{23}$$

Moreover, the air mass flow rate m_{O_2} (kg·s^{-1}) is obtained using (24) [81].

$$m_{O_2} = \left(\frac{M_{O_2}}{4 \cdot F} \right) \cdot \left(\frac{P_S}{V_{fc}} \right). \tag{24}$$

where M_{O_2} is the molar mass of oxygen (Kg·mol^{-1}). Additionally, the oxygen excess ratio μ_{O_2} is calculated as a function of the oxygen mass flow rate entering cathodes $m_{O_2,in}$ and m_{O_2} [57].

$$\mu_{O_2} = \frac{m_{O_2,in}}{m_{O_2}}, \tag{25}$$

$m_{O_2,in}$ is calculated using the mass flow rate of dry air $m_{a,in}$ in the cathode inlet and oxygen mass fraction $m_{O_2,fra}$,

$$m_{O_2,in} = m_{a,in} \cdot m_{O_2,fra}. \tag{26}$$

Additionally, during the operation of the stack, the rate of water production m_{H_2O} (kg·s^{-1}) is calculated using (27) [81]

$$m_{H_2O} = \left(\frac{M_{H_2O}}{2 \cdot F} \right) \cdot \left(\frac{P_S}{V_{fc}} \right). \tag{27}$$

where M_{H_2O} is the water molar mass (Kg·mol^{-1}).

Finally, the system PEMFC efficiency is obtained by (28) [81]

$$\eta = \frac{P_S}{m_{H_2O} \cdot LHV_{H_2}}, \tag{28}$$

where LHV_{H_2} is the lower heating power for hydrogen (120 J·kg^{-1}). This parameter is a measure of the available thermal energy produced by the combustion of hydrogen in a PEMFC. This parameter is calculated as the subtraction of the heat of the vaporization of water from the higher calorific value.

5. Electronic Circuit Designs for Electronic Emulators

Because the design of electronic circuits is important for the construction and implementation of electronic emulators, some electronic circuit designs are presented in this section.

The first ECM for PEMFC was proposed by Larminie et al. [82]. In this model, each electrode is represented by a parallel-connected capacitor, resistance, and voltage. The circuits reported in the literature are mainly focused on describing the voltage behavior of PEMFCs. For the design of electronic circuits, some authors have employed mathematical models [4,26–28,30,72,83–100], while others have chosen to describe the polarization curve taking into account the behavior of the electronic components [29,31,101].

5.1. Design of Electronic Circuits for Electrical Emulators

Examples of electronic circuit designs for electrical emulators are presented in this subsection for both equation-based designs and electronic components.

5.1.1. Design of Electronic Circuit Equation Based Electronic Circuits

To design an electronic circuit based on voltage–current equations, Nernst's voltage V_{ini} and the voltage drops must be considered (see (3) and (13)), as depicted in Figure 3.
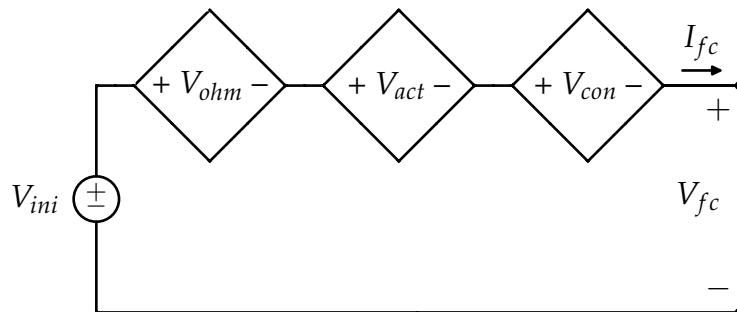

Figure 3. Schematic design of an electronic circuit using voltage–current equations.

An example of an electronic circuit is presented in Figure 4. In this case, the authors considered the nonlinear behavior of voltage drops V_{act} and V_{con}, which were modeled by a capacitor C (double-layer capacitance) and two resistances R_1 and R_2. One resistance R_{ohm} was used to model the voltage drop V_{ohm}. Additionally, in this example, the relationship of the PEMFC voltage with temperature and current is considered [35].
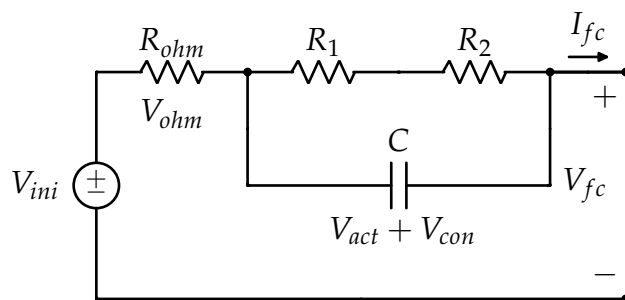

Figure 4. Example 1 of electronic circuit design for an electrical emulator [35].

Another design example of an electronic circuit is illustrated in Figure 5. This circuit consists of a PEMFC membrane resistance R_{ohm}, a parallel combination in series of one capacitor, and an impedance of a Faradic reaction formed of a charge transfer resistance R_{ct} and a specific electrochemical element of diffusion, which is also called a Warburg element (this element is estimated using a series combination of two parallel RCs) [83].
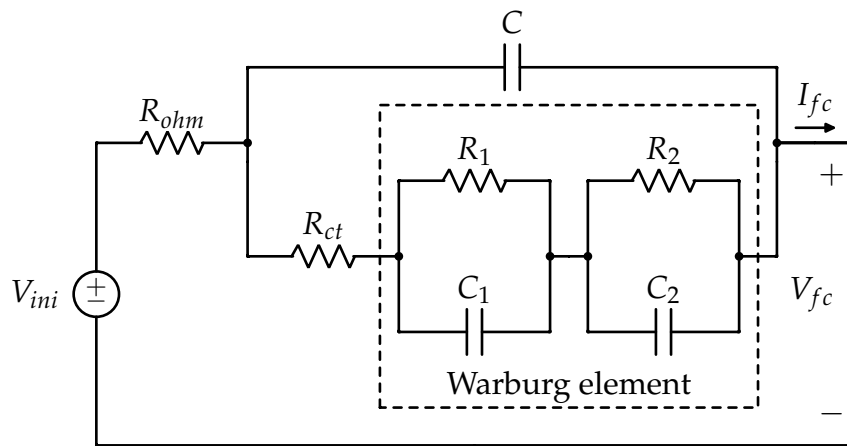

Figure 5. Example 2 of electronic circuit design for an electrical emulator [83].

One more example of electronic circuit design based on voltage–current equations is presented in [84]. The design includes the effects in both the anode (one capacitance C_a and two resistances $R_{act,a}$ and $R_{con,a}$) and cathode (one capacitance C_c and two resistances $R_{act,c}$ and $R_{con,c}$) sides, as shown in Figure 6.
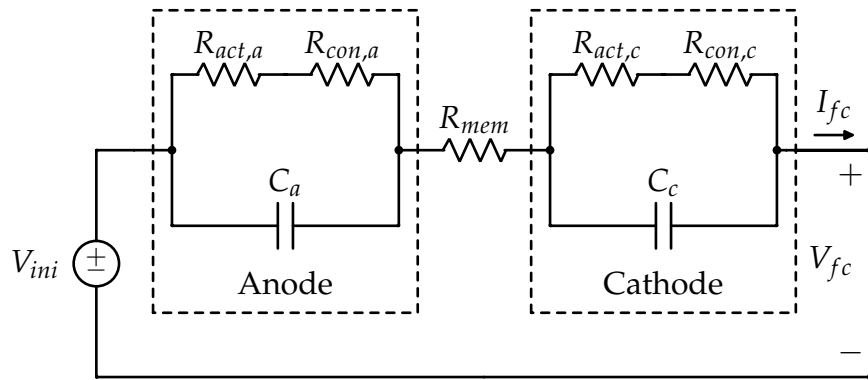

Figure 6. Example 3 of electronic circuit design for an electrical emulator [84].

However, as discussed in [84], compared with the cathode side, the anode side is barely affected by the activation and concentration voltage drops. To imitate this, a simplified ECM can be used, as shown in Figure 7.
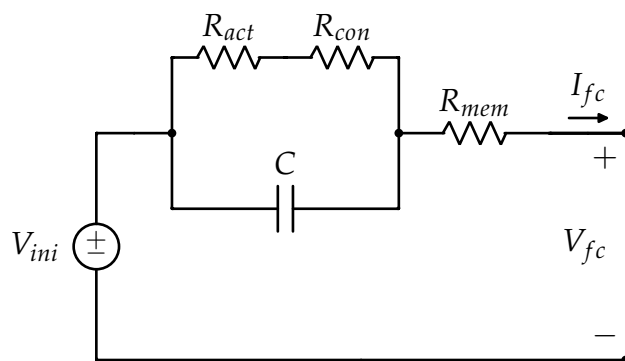

Figure 7. Example 4 of electronic circuit design for an electrical emulator [84].

5.1.2. Design of a Components-Based Electronic Circuit

In this example of electronic circuit design, the authors in [29,31] analyzed the behavior of the PEMFC polarization curve. Thus, they proposed a simplified electrical equivalent circuit built by a resistance R_{fc} in series with a DC voltage source, as shown in Figure 8.
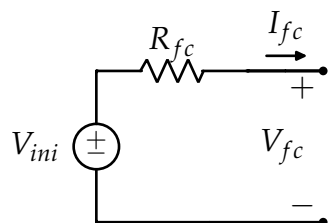

Figure 8. Example 5 of electronic circuit design for an electrical emulator [29,31].

5.2. *Design of Electronic Circuits for Heat Emulators*

In the studies reported so far, a controllable voltage source V_H and a resistive heater R_H form the heat electronic circuit. Additionally, the heat produced using this circuit is due to V_H (see (19)). the block of materials Rt_{Body} that must take into account the internal thermodynamic characteristics is positioned between R_H and the active cooling system, as shown in Figure 9. The internal heat capacitances and thermal conductivity of stack

membranes, gas diffusion layers, bipolar plates, and any other heat transfer physics that exist between the principal stack materials and the flowing coolant are some examples of these internal thermodynamic properties [11].
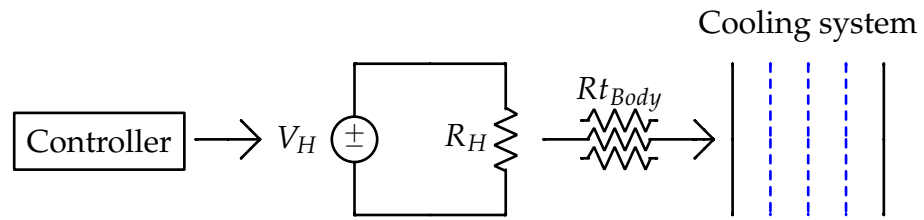

Figure 9. Example of electronic circuit design for a heat emulator [11].

6. Discussion

Figure 10 shows a comparison of the number of studies reported for models and designs of electronic circuits and the number of studies for validated PEMFC emulators per year. Before 2010, there was the highest number of papers on the development of electronic circuits that imitate the behavior of a PEMFC, while for emulators validated for PEMFC systems, the highest number of reported studies was between the years 2008 and 2020. This demonstrates the maturity that this technology has achieved in recent years.
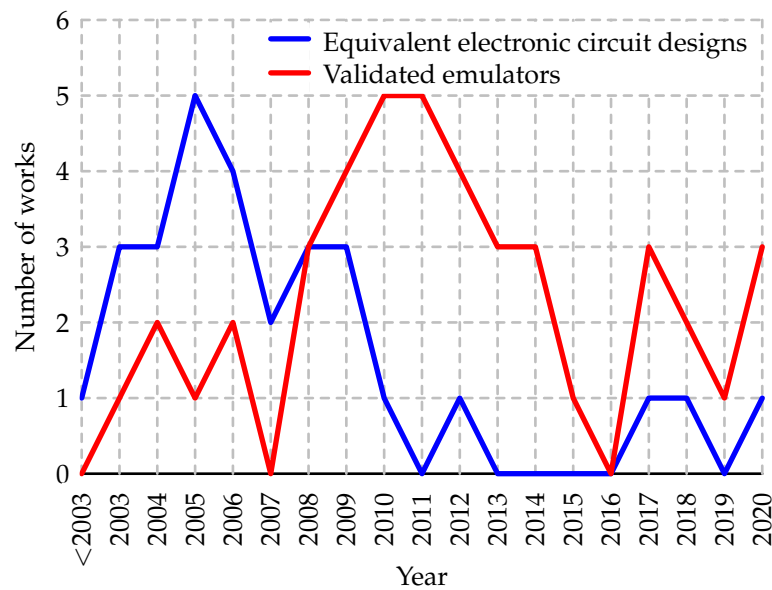

Figure 10. Evolution of the number of studies on electronic circuit designs and validated emulators per year.

Figure 11 illustrates a summary of this work. For electronic emulators (electrical and heat), controllers and mathematical models (simulation) need to be connected to them to obtain reliable measurements of a PEMFC system. For pseudo emulators, adequate scaling is needed for a small PEMFC to collect data from a reduced PEMFC system; later, these data are scaled to a real PEMFC system. However, in addition to the different parameters proposed in this review, it is necessary to take into consideration the different cooling methods used for the development of emulators and complex simulations [102,103], which are usually air cooling for PEMFCs less than 5 kW and coolant cooling for PEMFCs with power greater than 5 kW. Therefore, the temperature parameter of the PEMFC and the end purpose of the emulator are important factors to consider when developing one. Figure 11 shows the methods used to validate PEMFC emulators in general (i.e., through a comparison with data from a real PEMFC system and the HIL method).
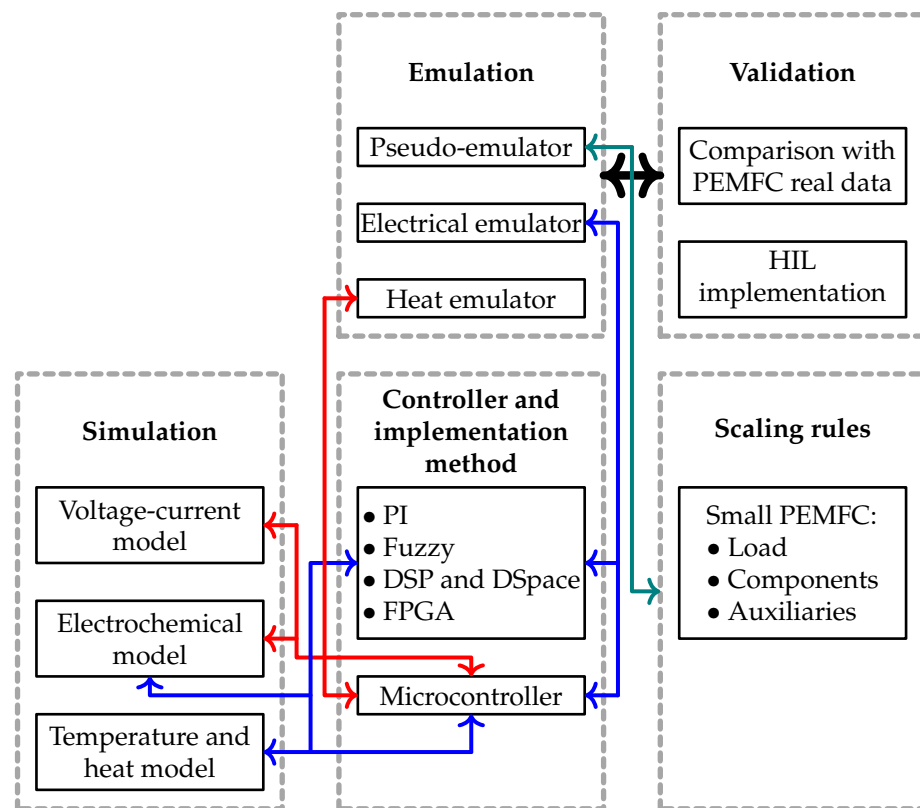
Figure 11. Diagram of the interactions of the different types of emulators with their components for proper operation.

7. Conclusions

PEMFC emulators are a valuable tool for developing PEMFC systems. This is because emulators reduce experimental cost, labor time, and installation space in the early stages of research, plus there is no risk of damaging the PEMFC system. Additionally, the PEMFC emulators presented in this paper can be widely used in various microgrid and hybrid energy storage simulators, where a fuel cell is an object (black box) in which input and output current parameters are read without considering the internal processes of the PEMFC.

This review presented a study of the different types of emulators for PEMFC (pseudo and electronic emulators). Electronic emulators have been developed in previous studies (development of ECMs); for their proper functioning, different types of controllers have been used. For pseudo emulators, an adequate reduction of the PEMFC system is necessary, which can be expensive. For the validation of PEMFC emulators, the data comparison method and the HIL method are generally used.

Different mathematical models were also presented for PEMFC systems. These models represent the simulated part of the system and, together with a PEMFC emulator, it is possible to obtain complete and reliable measurements of the entire system. Additionally, electrical circuit designs were presented to show the electrical components needed to build an electrical emulator (resistors, capacitors, and voltage sources). Therefore, this review supports the development of new PEMFC emulators.

Abbreviations

The following abbreviations are used in this manuscript:

DSP	Digital Signal Processor
ECM	Electronic Circuit Model
FC	Fuel Cell
FPGA	Field-Programmable Gate Array
HIL	Hardware-in-a-Loop
MDPI	Multidisciplinary Digital Publishing Institute
PEMFC	Proton Exchange Membrane Fuel Cell
PI	Proportional-Integral
PWM	Pulse Width Modulator

References

1. Zhang, H.; Sun, C.; Ge, M. Review of the Research Status of Cost-Effective Zinc–Iron Redox Flow Batteries. *Batteries* **2022**, *8*, 202. [CrossRef]
2. Albarbar, A.; Alrweq, M. *Introduction and Background*; Springer International Publishing: Cham, Switzerland, 2018; Chapter 1, pp. 1–8. [CrossRef]
3. Sopian, K.; Wan Daud, W.R. Challenges and future developments in proton exchange membrane fuel cells. *Renew. Energy* **2006**, *31*, 719–727. [CrossRef]
4. Larminie, J.; Dicks, A. *Introduction, Fuel Cell Systems Explained*, 2nd ed.; John Wiley & Sons, Ltd.: Hoboken, NJ, USA, 2003; Chapter 1, pp. 1–24. [CrossRef]
5. Barhate, S.; Mudhalwadkar, R. Portable fuel cell system emulator as a hardware-in-loop setup. In Proceedings of the International Conference on Communication & Information Processing (ICCIP) 2020, Tokyo, Japan, 27–29 November 2020; pp. 1–8. [CrossRef]
6. Daud, W.; Rosli, R.; Majlan, E.; Hamid, S.; Mohamed, R.; Husaini, T. Pem fuel cell system control: A review. *Renew. Energy* **2017**, *113*, 620–638. [CrossRef]
7. Jawad, N.H.; Yahya, A.A.; Al-Shathr, A.R.; Salih, H.G.; Rashid, K.T.; Al-Saadi, S.; AbdulRazak, A.A.; Salih, I.K.; Zrelli, A.; Alsalhy, Q.F. Fuel cell types, properties of membrane, and operating conditions: A review. *Sustainability* **2022**, *14*, 14653. [CrossRef]
8. Mao, L.; Jackson, L.; Huang, W.; Li, Z.; Davies, B. Polymer electrolyte membrane fuel cell fault diagnosis and sensor abnormality identification using sensor selection method. *J. Power Sources* **2020**, *447*, 227394. [CrossRef]
9. Tongroon, M.; Putrasari, Y.; Thongchai, S. Influence of engine operating conditions on effect of ethanol combined with biodiesel in ternary blends on combustion behavior in a compression ignition engine. *J. Mech. Sci. Technol.* **2023**, *37*, 1. [CrossRef]
10. Marsala, G.; Pucci, M.; Vitale, G.; Cirrincione, M.; Miraoui, A. A prototype of a fuel cell pem emulator based on a buck converter. *Appl. Energy* **2009**, *86*, 2192–2203. [CrossRef]
11. Kwan, T.H.; Yao, Q. A cost effective experimental emulator for fuel cell based combined heat and power systems. *Energy Procedia* **2019**, *158*, 1437–1448. [CrossRef]
12. Cirrincione, M.; Piazza, M.C.D.; Marsala, G.; Pucci, M.; Vitale, G. Real time simulation of renewable sources by model-based control of dc/dc converters. In Proceedings of the 2008 IEEE International Symposium on Industrial Electronics, Cambridge, UK, 30 June–2 July 2008; pp. 1548–1555. [CrossRef]
13. Gao, F.; Blunier, B.; Bouquain, D.; Miraoui, A.; Moudni, A.E. Polymer electrolyte fuel cell stack emulator for automotive hardware-in-the-loop applications. In Proceedings of the 2009 IEEE Vehicle Power and Propulsion Conference, Dearborn, MI, USA, 7–11 September 2009; pp. 998–1004. [CrossRef]
14. Gebregergis, A.; Pillay, P. Implementation of fuel cell emulation on dsp and dspace controllers in the design of power electronic converters. *IEEE Trans. Ind. Appl.* **2010**, *46*, 285–294. [CrossRef]
15. Voottipruex, K.; Sangswang, A.; Naetiladdanon, S.; Mujjalinvimut, E.; Wongyoa, N. Pem fuel cell emulator based on dynamic model with relative humidity calculation. In Proceedings of the 2017 14th International Conference on Electrical Engineering/Electronics, Computer, Telecommunications and Information Technology (ECTI-CON), Phuket, Thailand, 27–30 June 2017; pp. 529–532. [CrossRef]

16. Kartal, F.; Özveren, U. Investigation of an integrated circulating fluidized bed gasifier/steam turbine/proton exchange membrane (pem) fuel cell system for torrefied biomass and modeling with artificial intelligence approach. *Energy Convers. Manag.* **2022**, *263*, 115718. [CrossRef]

17. Zhang, Z.; Zhang, J.; Hu, S.; Zhang, T. An effective equivalent stiffness model combined with equivalent beam model to predict the contact pressure distribution for a large pem fuel cell stack. *Int. J. Hydrogen Energy* **2022**, *48*, 11431–11441. [CrossRef]

18. Gößling, S.; Nickig, N.; Bahr, M. 2-d + 1-d pem fuel cell model for fuel cell system simulations. *Int. J. Hydrogen Energy* **2021**, *46*, 34874–34882. [CrossRef]

19. Bernhard, D.; Kadyk, T.; Kirsch, S.; Scholz, H.; Krewer, U. Model-assisted analysis and prediction of activity degradation in pem-fuel cell cathodes. *J. Power Sources* **2023**, *562*, 232771. [CrossRef]

20. Kulikovsky, A. A model–based analysis of pem fuel cell distribution of relaxation times. *Electrochim. Acta* **2022**, *429*, 141046. [CrossRef]

21. Bagherabadi, K.B.; Skjong, S.; Pedersen, E. Dynamic modelling of pem fuel cell system for simulation and sizing of marine power systems. *Int. J. Hydrogen Energy* **2022**, *47*, 17699–17712. [CrossRef]

22. Kulikovsky, A. Analytical model for pem fuel cell concentration impedance. *J. Electroanal. Chem.* **2021**, *899*, 115672. [CrossRef]

23. Omran, A.; Lucchesi, A.; Smith, D.; Alaswad, A.; Amiri, A.; Wilberforce, T.; Sodré, J.R.; Olabi, A. Mathematical model of a proton-exchange membrane (pem) fuel cell. *Int. J. Thermofluids* **2021**, *11*, 100110. [CrossRef]

24. Li, Y.; Zhou, Z.; Liu, X.; Wu, W.-T. Modeling of pem fuel cell with thin mea under low humidity operating condition. *Appl. Energy* **2019**, *242*, 1513–1527. [CrossRef]

25. Qin, Y.; Ma, S.; Chang, Y.; Liu, Y.; Yin, Y.; Zhang, J.; Liu, Z.; Jiao, K.; Du, Q. Modeling the membrane/cl delamination with the existence of cl crack under rh cycling conditions of pem fuel cell. *Int. J. Hydrogen Energy* **2021**, *46*, 8722–8735. [CrossRef]

26. Runtz, K.; Lyster, M. Fuel cell equivalent circuit models for passive mode testing and dynamic mode design. In Proceedings of the Canadian Conference on Electrical and Computer Engineering, Saskatoon, SK, Canada, 1–4 May 2005; pp. 794–797. [CrossRef]

27. Yu, D.; Yuvarajan, S. Electronic circuit model for proton exchange membrane fuel cells. *J. Power Sources* **2005**, *142*, 238–242. [CrossRef]

28. Garnier, J.; Pera, M.; Hissel, D.; Harel, F.; Candusso, D.; Glandut, N.; Diard, J.; Bernardinis, A.D.; Kauffmann, J.; Coquery, G. Dynamic pem fuel cell modeling for automotive applications. In Proceedings of the 2003 IEEE 58th Vehicular Technology Conference. VTC 2003-Fall (IEEE Cat. No.03CH37484), Orlando, FL, USA, 6–9 October 2003; Volume 5, pp. 3284–3288. [CrossRef]

29. Choi, W.; Howze, J.; Enjeti, P. Development of an equivalent circuit model of a fuel cell to evaluate the effects of inverter ripple current. *J. Power Sources* **2006**, *158*, 1324–1332, papers from the 6th International Conference on Lead-Acid Batteries (LABAT 2005, Varna, Bulgaria) and the 11th Asian Battery Conference (11 ABC, Ho Chi Minh City, Vietnam) together with regular papers. [CrossRef]

30. Zhang, Z.; Huang, X.; Jiang, J.; Wu, B. An improved dynamic model considering effects of temperature and equivalent internal resistance for pem fuel cell power modules. *J. Power Sources* **2006**, *161*, 1062–1068. [CrossRef]

31. Choi, W.; Enjeti, P.; Howze, J. Development of an equivalent circuit model of a fuel cell to evaluate the effects of inverter ripple current. In Proceedings of the Nineteenth Annual IEEE Applied Power Electronics Conference and Exposition, 2004. APEC '04, Anaheim, CA, USA, 22–26 February 2004; Volume 1, pp. 355–361. [CrossRef]

32. Parker-Allotey, N.; Bryant, A.; Palmer, P. The application of fuel cell emulation in the design of an electric vehicle powertrain. In Proceedings of the 2005 IEEE 36th Power Electronics Specialists Conference, Dresden, Germany, 16 June 2005; pp. 1869–1874. [CrossRef]

33. Lee, T.-W.; Kim, S.-H.; Yoon, Y.-H.; Jang, S.-J.; Won, C.-Y. A 3 kw fuel cell generation system using the fuel cell simulator. In Proceedings of the 2004 IEEE International Symposium on Industrial Electronics, Scottsdale, AZ, USA, 10–13 May 2004; Volume 2, pp. 833–837. [CrossRef]

34. Rezzak, D.; Khoucha, F.; Benbouzid, M.; Kheloui, A.; Mamoune, A. A dc-dc converter-based pem fuel cell system emulator. In Proceedings of the 2011 International Conference on Power Engineering, Energy and Electrical Drives, Malaga, Spain, 11–13 May 2011; pp. 1–6. [CrossRef]

35. García-Vite, P.M.; Reyes-García, B.L.; Valdez-Hernández, C.L.; Martínez-Salazar, A. Microcontroller-based emulation of a pem fuel cell. *Int. J. Hydrogen Energy* **2020**, *45*, 13767–13776. [CrossRef]

36. Restrepo, C.; Konjedic, T.; Garces, A.; Calvente, J.; Giral, R. Identification of a proton-exchange membrane fuel cell's model parameters by means of an evolution strategy. *IEEE Trans. Ind. Inform.* **2015**, *11*, 548–559. [CrossRef]

37. Sanchez, V.M.; Barbosa, R.; Arriaga, L.; Ramirez, J.M. Real time control of air feed system in a pem fuel cell by means of an adaptive neural-network. *Int. J. Hydrogen Energy* **2014**, *39*, 16750–16762. [CrossRef]

38. Paja, C.A.R.; Nevado, A.R.; Castillón, R.G.; Martinez-Salamero, L.; Saenz, C.I.S. Switching and linear power stages evaluation for pem fuel cell emulation. *Int. J. Circuit Theory Appl.* **2011**, *39*, 475–499. [CrossRef]

39. Marsala, G.; Bouquin, D.; Pukrushpan, J.T.; Pucci, M.; Cirrincione, G.; Vitale, G.; Miraoui, A. A neural inverse control of a pem-fc system by the generalized mapping regressor (gmr). In Proceedings of the 2008 IEEE Industry Applications Society Annual Meeting, Edmonton, AB, Canada, 5–9 October 2008; pp. 1–12. [CrossRef]

40. Pinto, F.R.P.; Vega-Leal, A.P. A test of hil cots technology for fuel cell systems emulation. *IEEE Trans. Ind. Electron.* **2010**, *57*, 1237–1244. [CrossRef]

41. Sanchez, V.; Chan, F.; Ramírez, J.M.; Rosas-Caro, J.C. Fuel cell emulator based on interleaved synchronous buck converter. In Proceedings of the 2012 IEEE Energy Conversion Congress and Exposition (ECCE), Raleigh, NC, USA, 15–20 September 2012; pp. 4464–4470. [CrossRef]

42. Gauchia, L.; Sanz, J. A per-unit hardware-in-the-loop simulation of a fuel cell/battery hybrid energy system. *IEEE Trans. Ind. Electron.* **2010**, *57*, 1186–1194. [CrossRef]

43. Lim, J.-G.; Kim, S.-H.; Seo, E.-K.; Shin, H.-B.; Chung, S.-K.; Lee, H.-W. Implementation of fuel cell dynamic simulator. In Proceedings of the 2006 37th IEEE Power Electronics Specialists Conference, Jeju, Republic of Korea, 18–22 June 2006; pp. 1–5. [CrossRef]

44. Gao, F.; Blunier, B.; Simões, M.G.; Miraoui, A. Pem fuel cell stack modeling for real-time emulation in hardware-in-the-loop applications. *IEEE Trans. Energy Convers.* **2011**, *26*, 184–194. [CrossRef]

45. Gao, F.; Chrenko, D.; Blunier, B.; Bouquain, D.; Miraoui, A. Multi-rates fuel cell emulation with spatial reduced real-time fuel cell modelling. In Proceedings of the 2011 IEEE Industry Applications Society Annual Meeting, Orlando, FL, USA, 9–13 October 2011; pp. 1–8. [CrossRef]

46. Liu, J.; Laghrouche, S.; Ahmed, F.-S.; Wack, M. Pem fuel cell air-feed system observer design for automotive applications: An adaptive numerical differentiation approach. *Int. J. Hydrogen Energy* **2014**, *39*, 17210–17221. [CrossRef]

47. Lemeš, Z.; Vath, A.; Hartkopf, T.; Mäncher, H. Dynamic fuel cell models and their application in hardware in the loop simulation. *J. Power Sources* **2006**, *154*, 386–393. [CrossRef]

48. Restrepo, C.; Ramos-Paja, C.; Giral, R.; Calvente, J.; Romero, A. Fuel cell emulator for oxygen excess ratio estimation on power electronics applications. *Comput. Electr. Eng.* **2012**, *38*, 926–937. [CrossRef]

49. Das, H.S.; Tan, C.W.; Yatim, A.; Muhamad, N.D.b. Proton exchange membrane fuel cell emulator using pi controlled buck converter. *Int. J. Power Electron. Drive Syst. (IJPEDS)* **2017**, *8*, 462–469. [CrossRef]

50. Samosir, A.S.; Anwari, M.; Yatim, A.H.M. A simple pem fuel cell emulator using electrical circuit model. In Proceedings of the 2010 Conference Proceedings IPEC, Singapore, 27–29 October 2010; pp. 881–885. [CrossRef]

51. Karami, N.; Outbib, R.; Moubayed, N. A low-cost microcontroller based 500-watt pem fuel cell emulator. In Proceedings of the 2012 IEEE International Systems Conference SysCon, Vancouver, BC, Canada, 19–22 March 2012; pp. 1–4. [CrossRef]

52. Ramos-Paja, C.; Jaramillo-Matta, A.; Pérez-Rojas, A.; Antonio, E. Design and implementation of a pem fuel cell emulator for static and dynamic behavior. *Dyna* **2011**, *78*, 1–12. Available online: https://www.redalyc.org/articulo.oa?id=49622401013 (accessed on 23 March 2023).

53. Premkumar, K.; Vishnupriya, M.; Thamizhselvan, T.; Sanjeevikumar, P.; Manikandan, B. Pso optimized pi controlled dc-dc buck converter-based proton-exchange membrane fuel cell emulator for testing of mppt algorithm and battery charger controller. *Int. Trans. Electr. Energy Syst.* **2021**, *31*, e12754. [CrossRef]

54. Ramos-Paja, C.; Romero, A.; Giral, R.; Vidal-Idiarte, E.; Martinez-Salamero, L. Fuzzy-based modelling technique for pemfc electrical power generation systems emulation. *IET Power Electron.* **2009**, *2*, 241–255. Available online: https://digital-library.theiet.org/content/journals/10.1049/iet-pel.2008.0008 (accessed on 23 March 2023). [CrossRef]

55. de Beer, C.; Barendse, P.; Khan, A. Development of an ht pem fuel cell emulator using a multiphase interleaved dc–dc converter topology. *IEEE Trans. Power Electron.* **2013**, *28*, 1120–1131. [CrossRef]

56. Lindahl, P.A.; Shaw, S.R.; Leeb, S.B. Fuel cell stack emulation for cell and hardware-in-the-loop testing. *IEEE Trans. Instrum. Meas.* **2018**, *67*, 2143–2152. [CrossRef]

57. Benyahia, N.; Rekioua, T.; Benamrouche, N.; Bousbaine, A. Fuel cell emulator for supercapacitor energy storage applications. *Electr. Power Components Syst.* **2013**, *41*, 569–585. [CrossRef]

58. Jung, J.-H.; Ahmed, S.; Enjeti, P. Pem fuel cell stack model development for real-time simulation applications. *IEEE Trans. Ind. Electron.* **2011**, *58*, 4217–4231. [CrossRef]

59. Boscaino, V.; Miceli, R.; Capponi, G. Matlab-based simulator of a 5 kw fuel cell for power electronics design. *Int. J. Hydrogen Energy* **2013**, *38*, 7924–7934. [CrossRef]

60. Bojoi, R.; Tenconi, A.; Vaschetto, S.; Colasante, L.; Delmastro, A. Power electronics of a real-time emulator of pem fuel cell systems. In Proceedings of the 2009 International Conference on Clean Electrical Power, Capri, Italy, 9–11 June 2009; pp. 338–343. [CrossRef]

61. Boscaino, V.; Capponi, G.; Marino, F. Fpga implementation of a fuel cell emulator. *SPEEDAM* **2010**, *2010*, 1297–1301. [CrossRef]

62. Sirisukprasert, S.; Saengsuwan, T. The modeling and control of fuel cell emulators. In Proceedings of the 2008 5th International Conference on Electrical Engineering/Electronics, Computer, Telecommunications and Information Technology, Krabi, Thailand, 14–17 May 2008; Volume 2, pp. 985–988. [CrossRef]

63. Flores-Bahamonde, F.; Rivera, M.; Baier, C.; Calvente, J.; Giral, R.; Restrepo, C. Dc transformer based on the versatile dc-dc noninverting buck-boost converter for fuel cell emulation. In Proceedings of the 2017 IEEE Southern Power Electronics Conference (SPEC), Puerto Varas, Chile, 4–7 December 2017; pp. 1–6. [CrossRef]

64. Alberro, M.; Marzo, F.; Manso, A.; Domínguez, V.; Barranco, J.; Garikano, X. Electronic modeling of a pemfc with logarithmic amplifiers. *Int. J. Hydrogen Energy* **2015**, *40*, 3708–3718. [CrossRef]

65. Correa, J.; Farret, F.; Gomes, J.; Simoes, M. Simulation of fuel-cell stacks using a computer-controlled power rectifier with the purposes of actual high-power injection applications. *IEEE Trans. Ind. Appl.* **2003**, *39*, 1136–1142. [CrossRef]

66. Lee, T.-W.; Lee, B.-K.; Jang, S.-J.; Kim, S.-H.; Won, C.-Y. Development of a 3 kw fuel cell generation system with an active fuel cell simulator: Topology, control, and design. In Proceedings of the 2004 IEEE 35th Annual Power Electronics Specialists Conference (IEEE Cat. No.04CH37551), Aachen, Germany, 20–25 June 2004; Volume 6, pp. 4743–4748. [CrossRef]

67. Kwan, T.H.; Wu, X.; Yao, Q. Integrated teg-tec and variable coolant flow rate controller for temperature control and energy harvesting. *Energy* **2018**, *159*, 448–456. [CrossRef]

68. Albarbar, A.; Alrweq, M. *Proton Exchange Membrane Fuel Cells: Review*; Springer International Publishing: Cham, Switzerland, 2018; Chapter 2, pp. 9–29. [CrossRef]

69. Pukrushpan, J.T.; Stefanopoulou, A.G.; Peng, H. *Background and Introduction*; Springer: London, UK, 2004; Chapter 1, pp. 1–13. [CrossRef]

70. Sun, C.; Negro, E.; Vezzu, K.; Pagot, G.; Cavinato, G.; Nale, A.; Bang, Y.H.; Noto, V.D. Hybrid inorganic-organic proton-conducting membranes based on SPEEK doped with WO3 nanoparticles for application in vanadium redox flow batteries. *Electrochim. Acta* **2019**, *309*, 311–325. [CrossRef]

71. Sun, C.-Y.; Zhang, H. Investigation of Nafion series membranes on the performance of iron-chromium redox flow battery. *Int. J. Energy Res.* **2019**, *43*, 8739–8752. [CrossRef]

72. Puranik, S.V.; Keyhani, A.; Khorrami, F. State-space modeling of proton exchange membrane fuel cell. *IEEE Trans. Energy Convers.* **2010**, *25*, 804–813. [CrossRef]

73. Acharya, P.; Enjeti, P.; Pitel, I. An advanced fuel cell simulator. In Proceedings of the Nineteenth Annual IEEE Applied Power Electronics Conference and Exposition, APEC '04, Anaheim, CA, USA, 22–26 February 2004; Volume 3, pp. 1554–1558. [CrossRef]

74. Ordonez, M.; Iqbal, M.; Quaicoe, J. Dev elopment of a fuel cell simulator based on an experimentally derived model. In Proceedings of the Canadian Conference on Electrical and Computer Engineering, Saskatoon, SK, Canada, 1–4 May 2005; pp. 1449–1452. [CrossRef]

75. Ordonez, M.; Iqbal, M.; Quaicoe, J. A novel fuel cell simulator. In Proceedings of the 2005 IEEE 36th Power Electronics Specialists Conference, Dresden, Germany, 16 June 2005; pp. 178–184. [CrossRef]

76. Yang, F.; Zhu, X.-J.; Cao, G.-Y. Nonlinear fuzzy modeling of a mcfc stack by an identification method. *J. Power Sources* **2007**, *166*, 354–361. [CrossRef]

77. Pukrushpan, J.T.; Stefanopoulou, A.G.; Peng, H. *Fuel Cell System Model: Fuel Cell Stack*; Springer: London, UK, 2004; Chapter 3, pp. 31–56. [CrossRef]

78. Musio, F.; Tacchi, F.; Omati, L.; Stampino, P.G.; Dotelli, G.; Limonta, S.; Brivio, D.; Grassini, P. Pemfc system simulation in matlab-simulink® environment. *Int. J. Hydrogen Energy* **2011**, *36*, 8045–8052. [CrossRef]

79. Sankar, K.; Aguan, K.; Jana, A.K. A proton exchange membrane fuel cell with an airflow cooling system: Dynamics, validation and nonlinear control. *Energy Convers. Manag.* **2019**, *183*, 230–240. [CrossRef]

80. Buasri, P.; Salameh, Z. An electrical circuit model for a proton exchange membrane fuel cell (pemfc). In Proceedings of the 2006 IEEE Power Engineering Society General Meeting, Montreal, QC, Canada, 18–22 June 2006; p. 6. [CrossRef]

81. San Martin, J.; Zamora, I.; San Martin, J.; Aperribay, V.; Torres, E.; Eguia, P. Influence of the rated power in the performance of different proton exchange membrane (pem) fuel cells. *Energy* **2010**, *35*, 1898–1907. [CrossRef]

82. Larminie, J. Current interrupt techniques for circuit modelling. In Proceedings of the IEE Colloquium on Electrochemical Measurement, London, UK, 17 March 1994; pp. 1–6.

83. Fardoun, A.A.; Hejase, H.A.; Al-Marzouqi, A.; Nabag, M. Electric circuit modeling of fuel cell system including compressor effect and current ripples. *Int. J. Hydrogen Energy* **2017**, *42*, 1558–1564. [CrossRef]

84. Mohammadi, A.; Cirrincione, G.; Djerdir, A.; Khaburi, D. A novel approach for modeling the internal behavior of a pemfc by using electrical circuits. *Int. J. Hydrogen Energy* **2018**, *43*, 11539–11549. [CrossRef]

85. Ferrero, R.; Marracci, M.; Prioli, M.; Tellini, B. Simplified model for evaluating ripple effects on commercial pem fuel cell. *Int. J. Hydrogen Energy* **2012**, *37*, 13462–13469. [CrossRef]

86. Wang, C.; Nehrir, M.; Shaw, S. Dynamic models and model validation for pem fuel cells using electrical circuits. *IEEE Trans. Energy Convers.* **2005**, *20*, 442–451. [CrossRef]

87. Rubio, M.; Urquia, A.; Dormido, S. Diagnosis of pem fuel cells through current interruption. *J. Power Sources* **2007**, *171*, 670–677. [CrossRef]

88. Famouri, P.; Gemmen, R. Electrochemical circuit model of a pem fuel cell. In Proceedings of the 2003 IEEE Power Engineering Society General Meeting (IEEE Cat. No.03CH37491), Toronto, ON, Canada, 13–17 July 2003; Volume 3, pp. 1436–1440. [CrossRef]

89. Yu, D.; Yuvarajan, S. A novel circuit model for pem fuel cells. In Proceedings of the Nineteenth Annual IEEE Applied Power Electronics Conference and Exposition, APEC '04, Anaheim, CA, USA, 22–26 February 2004; Volume 1, pp. 362–366. [CrossRef]

90. Adzakpa, K.P.; Agbossou, K.; DubÉ, Y.; Dostie, M.; Fournier, M.; Poulin, A. Pem fuel cells modeling and analysis through current and voltage transient behaviors. *IEEE Trans. Energy Convers.* **2008**, *23*, 581–591. [CrossRef]

91. Khan, M.J.; Iqbal, M.T. Modelling and analysis of electro-chemical, thermal, and reactant flow dynamics for a pem fuel cell system. *Fuel Cells* **2005**, *5*, 463–475. [CrossRef]

92. Correa, J.; Farret, F.; Popov, V.; Simoes, M. Sensitivity analysis of the modeling parameters used in simulation of proton exchange membrane fuel cells. *IEEE Trans. Energy Convers.* **2005**, *20*, 211–218. [CrossRef]

93. Qingshan, X.; Nianchun, W.; Ichiyanagi, K.; Yukita, K. Pem fuel cell modeling and parameter influences of performance evaluation. In Proceedings of the 2008 Third International Conference on Electric Utility Deregulation and Restructuring and Power Technologies, Nanjing, China, 6–9 April 2008; pp. 2827–2832. [CrossRef]

94. Lee, D.-J.; Wang, L. Dynamic and steady-state performance of pem fuel cells under various loading conditions. In Proceedings of the 2007 IEEE Power Engineering Society General Meeting, Tampa, FL, USA, 24–28 June 2007; pp. 1–8. [CrossRef]

95. Lazarou, S.; Pyrgioti, E.; Alexandridis, A.T. A simple electric circuit model for proton exchange membrane fuel cells. *J. Power Sources* **2009**, *190*, 380–386. [CrossRef]

96. Andujar, J.; Segura, F.; Vasallo, M. A suitable model plant for control of the set fuel cell–dc/dc converter. *Renew. Energy* **2008**, *33*, 813–826. [CrossRef]

97. Laffly, E.; Pera, M.-C.; Hissel, D. Dynamic model of a polymer electrolyte fuel cell power device. In Proceedings of the IECON 2006—32nd Annual Conference on IEEE Industrial Electronics, Paris, France, 7–10 November 2006; pp. 466–471. [CrossRef]

98. Brunetto, C.; Moschetto, A.; Tina, G. Pem fuel cell testing by electrochemical impedance spectroscopy. *Electr. Power Syst. Res.* **2009**, *79*, 17–26. [CrossRef]

99. Restrepo, C.; Torres, C.; Calvente, J.; Giral, R.; Leyva, R. Simulator of a pem fuel-cell stack based on a dynamic model. In Proceedings of the 2009 35th Annual Conference of IEEE Industrial Electronics, Porto, Portugal, 3–5 November 2009; pp. 2796–2801. [CrossRef]

100. Lan, T.; Strunz, K. Modeling of multi-physics transients in pem fuel cells using equivalent circuits for consistent representation of electric, pneumatic, and thermal quantities. *Int. J. Electr. Power Energy Syst.* **2020**, *119*, 105803. [CrossRef]

101. Page, S.; Krumdieck, S.; Al-Anbuky, A. Testing procedure for passive fuel cell state of health. In Proceedings of the Australasian Universities Power Engineering Conference (AUPEC 2004), Brisbane, Australia, 26–29 September 2004; pp. 1–6.

102. Forde, T.; Eriksen, J.; Pettersen, A.G.; Vie, P.J.S.; Ulleberg, O. Thermal integration of a metal hydride storage unit and a PEM fuel cell stack. *Int. J. Hydrogen Energy* **2009**, *34*, 6730–6739. [CrossRef]

103. Yiotis, A.G.; Kainourgiakis, M.E.; Charalambopoulou, G.C.; Stubos, A.K. A generic physical model for a thermally integrated high-temperature PEM fuel cell and sodium alanate tank system. *Int. J. Hydrogen Energy* **2015**, *40*, 14551–14561. [CrossRef]